International Immunopharmacology 72 (2019) 166–175

Contents lists available at ScienceDirect

International Immunopharmacology

journal homepage: www.elsevier.com/locate/intimp

Protective effects of tauroursodeoxycholic acid on lipopolysaccharide-induced cognitive impairment and neurotoxicity in mice

Xian Wu[a], Caihong Liu[a], Liang Chen[a], Yi-Feng Du[b], Mei Hu[a], Miranda N. Reed[b], Yan Long[a], Vishnu Suppiramaniam[b], Hao Hong[a,*], Su-Su Tang[a,*]

[a] Department of Pharmacology, Key Laboratory of Neuropsychiatric Diseases, China Pharmaceutical University, Nanjing 210009, China
[b] Department of Drug Discovery and Development, School of Pharmacy, Auburn University, Auburn, AL, USA

ARTICLE INFO

Keywords:
Tauroursodeoxycholic acid
TGR5
Lipopolysaccharide
Cognitive impairment
Neuroinflammation

ABSTRACT

Accumulating evidence has shown that tauroursodeoxycholic acid (TUDCA) is neuroprotective in different animal models of neurological diseases. However, whether TGR5 agonist TUDCA can improve lipopolysaccharide (LPS)-induced cognitive impairment in mice is less clear. Using a model of cognitive impairment with LPS (2.0 μg) we investigated the effects of TUDCA (200 or 400 μg) on cognitive dysfunction and neurotoxicity in mice. Both Morris water maze and Y-maze avoidance tests showed that TUDCA treatment significantly alleviated LPS-induced behavioral impairments. More importantly, we found that TUDCA treatment reversed TGR5 down-regulation, prevented neuroinflammation via inhibiting NF-κB signaling in the hippocampus of LPS-treated mice. Additionally, TUDCA treatment decreased LPS-induced apoptosis through decreasing TUNEL-positive cells and the overexpression of caspase-3, increasing the ratio of Bcl-2/Bax. TUDCA treatment also ameliorated synaptic plasticity impairments by increasing the ratio of mBDNF/proBDNF, the number of dendritic spines and the expression of synapse-associated proteins in the hippocampus. Our results indicated that TUDCA can improve cognitive impairment and neurotoxicity induced by LPS in mice, which is involved in TGR5-mediated NF-κB signaling.

1. Introduction

Alzheimer's disease (AD) is a most common type of dementia in aged people, and its primary character is cognitive and memory impairment [1,2]. Previous studies reported that hippocampal neuroinflammation can cause cognitive impairment [1]. Lipopolysaccharide (LPS) has been long known to induce neuroinflammation, hippocampal cell loss and memory deficits [3,4]. Single intracerebroventricle injection of LPS in mice can induce neuroinflammation, which is a valid model for cognitive dysfunction [5–7]. NF-κB pathway can regulate the transcription of inflammatory genes including the expression of pro-inflammatory cytokines [8]. In addition, neuroinflammation is thought to be associated with the upregulation of NF-κB [9]. There is enough evidence illustrating that a strong association between neuroinflammation and the activation of microglia as well as the production of proinflammatory cytokines [10,11]. It has been investigated that cognitive impairment induced by LPS is linked to apoptosis [12,13]. It is well known that brain-derived neurotrophic factor (BDNF) plays an important role in memory formation [14]. The BDNF gene deletion in the hippocampus impairs spatial learning [15]. Hippocampal dendritic spines are highly associated with cognitive function and synaptic plasticity [2]. Moreover, deficits in postsynaptic (PSD-95) and presynaptic (synaptophysin) proteins correlate with cognition decline in AD [16,17].

TGR5 is also known as G protein-coupled bile acid receptor 1 (Gpbar1), which has been shown to be expressed in the brain and is considered to be neuroprotective [18–20]. Activation of TGR5 by bile acids may regulate plasma glucose and attenuate diet-induced obesity [21,22]. Activation of TGR5 also exerts a protective effect against neuroinflammation [23]. TUDCA is an agonist of TGR5, which has been shown to have a neuroprotective effect in stroke, and amyotrophic lateral sclerosis patients [23–25]. In addition, TUDCA has also been revealed to alleviate apoptosis in neuron [23]. However, the impact of TUDCA on LPS-induced cognitive dysfunction is unknown. Thus, this study was aimed at uncovering the neuroprotective effects of TUDCA on cognitive impairment and neurotoxicity induced by LPS in mice.

* Corresponding authors at: Department of Pharmacology, China Pharmaceutical University, Nanjing 210009, China.
E-mail addresses: honghao@cpu.edu.cn (H. Hong), tang_susu@126.com (S.-S. Tang).

https://doi.org/10.1016/j.intimp.2019.03.065
Received 10 December 2018; Received in revised form 18 March 2019; Accepted 31 March 2019
Available online 12 April 2019

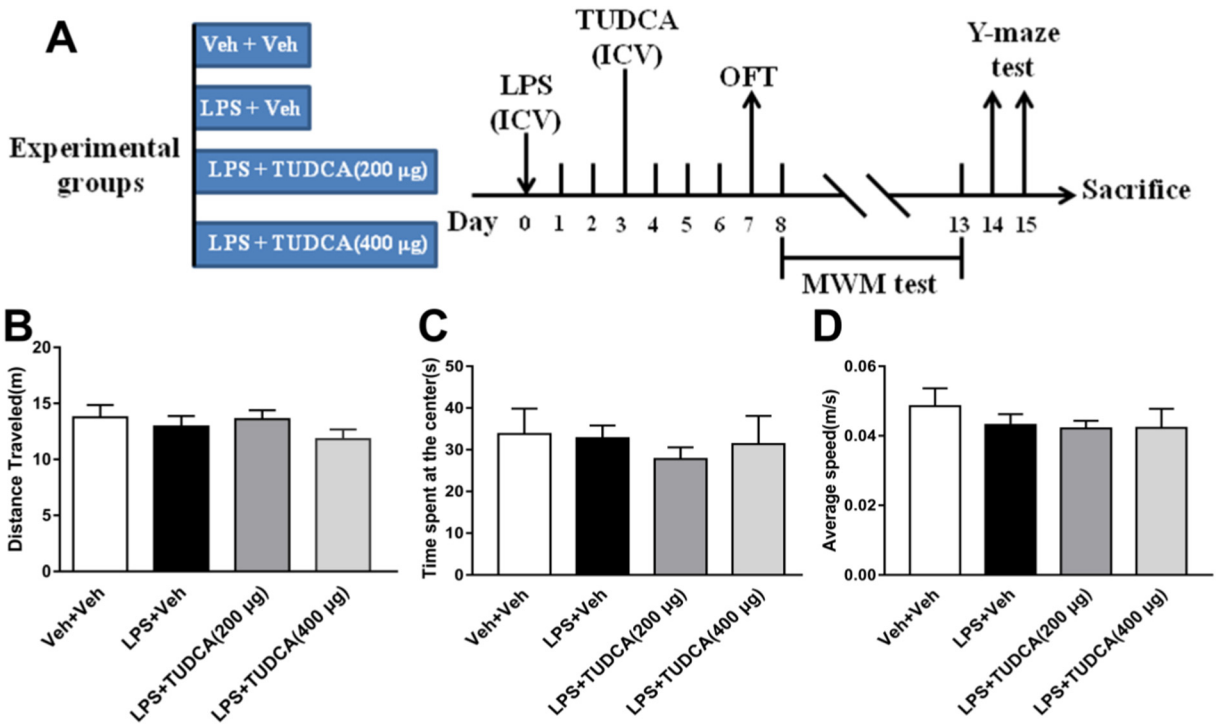

Fig. 1. Effects of TUDCA on LPS-treated mice in the locomotor activity test. (A) Animal groups and the schedule of the experiment. The locomotor activity test was evaluated for the following parameters: (B) the distance traveled, (C) the time spent in the center zone and (D) the average speed. Data are mean ± SEM, n = 12 mice/group.

2. Materials and methods

2.1. Animals and drug treatments protocol

Male ICR mice (weighing 22–25 g) were purchased from Yangzhou University Medical Center (Yangzhou, China). Mice were housed under a 12-h-light/dark cycle with ad libitum access to food and water. TUDCA was acquired from YuanYe BioScience Company Ltd. (Shanghai, China). LPS from Sigma Aldrich (serotype 05:B5, St. Louis, MO).

Stereotaxic surgery was conducted on mice anaesthetized with chloral hydrate (350 mg/kg, intraperitoneal injection). Mice were intracerebroventricular injection of LPS (0.4 μg/μl, 5 μl, i.c.v.) 3 days prior to intracerebroventricular injection of TUDCA (200 or 400 μg) [26] under the following coordinates: (0.5 mm posterior, ± 1.0 mm lateral, and 2.0 mm ventral from bregma) [7]. After surgery for 3 days, mice were undergone the behavioral tests in a quiet room (Fig. 1A). All experimental procedures that involved animals were carried out in accordance with the guidelines of the Institutional Animal Care and Use Committee of China.

2.2. Behavioral analysis

2.2.1. Locomotor activity

Locomotor activity of mice in the open field (50 cm wide × 50 cm deep × 50 cm high) was recorded during 5 min [27]. The variables recorded included the total distance, the time spent in the central squares and the average speed. After each trial, the apparatus was thoroughly cleaned with 5% ethyl alcohol to avoid odor clues.

2.2.2. Morris water maze

The Morris water maze test, which is used to evaluate the spatial learning and memory for rodents [28,29]. Four training sessions were performed on each mice per day. During the visible platform (with flag, days 1–2) test, an escape platform (9 cm in diameter) was located in one of the four quadrants of the pool. The hidden-platform (without flag, days 3–5) test was used to determine the retention of memory to find the platform. Finding the platform was defined as staying on it for at least 10 s before the acquisition time of 90 s ended. When the mice failed to find the platform in the limited time (90 s), it should be guided to the platform for 30 s. The mice received a 90-s probe trial on the sixth day (without platform). The escape latency, the time spent in the previous platform quadrant, the number of mouse traversing the platform and the average swimming speed were recorded.

2.2.3. Y-maze avoidance

The trial was conducted for 2 consecutive days [13]. On day 1 (learning trial), each mouse was allowed to explore freely for 5 min. After 5 min, a foot stimulation (2 Hz, 125 ms, 10 V) was made available in two of the arms while one arm was left shock-free. The safe arm was demarcated from the other two by a light. Only if the animal entered the safe arm and stayed for 30 s, the training would be stopped and a correct choice would be recorded. If the mice do not enter this arm, they would be guided to the arm and allowed to stay for 30 s. On day 2 (testing trial), the same test procedure was followed on day 1 except 5-min habituation period. The number of correct choices (10 times) and the latency to enter the safe arm was recorded manually.

2.3. Western blotting assay

The method was carried out as described previously [28]. The protein sample (40 μg) was transferred to a PVDF membrane after separated electrophoretically in 8 or 12% sodium dodecyl sulfate (SDS) polyacrylamide gel. The following primary antibodies were used: TGR5 (1:1000 dilution, Abcam), TNF-α (1:500 dilution, Santa Cruz Biotechnology), IL-1β (1:1000 dilution, Santa Cruz Biotechnology), IL-6 (1:1000 dilution, Cell Signaling Technology), IL-10 (1:500 dilution, Affinity Biosciences), Iba1 (1:1000 dilution, Wako Pure Chemical Industries), caspase-3 (1:1000 dilution, Cell Signaling Technology), Bcl-2 (1:1000 dilution, Cell Signaling Technology), Bax (1:500 dilution, Cell

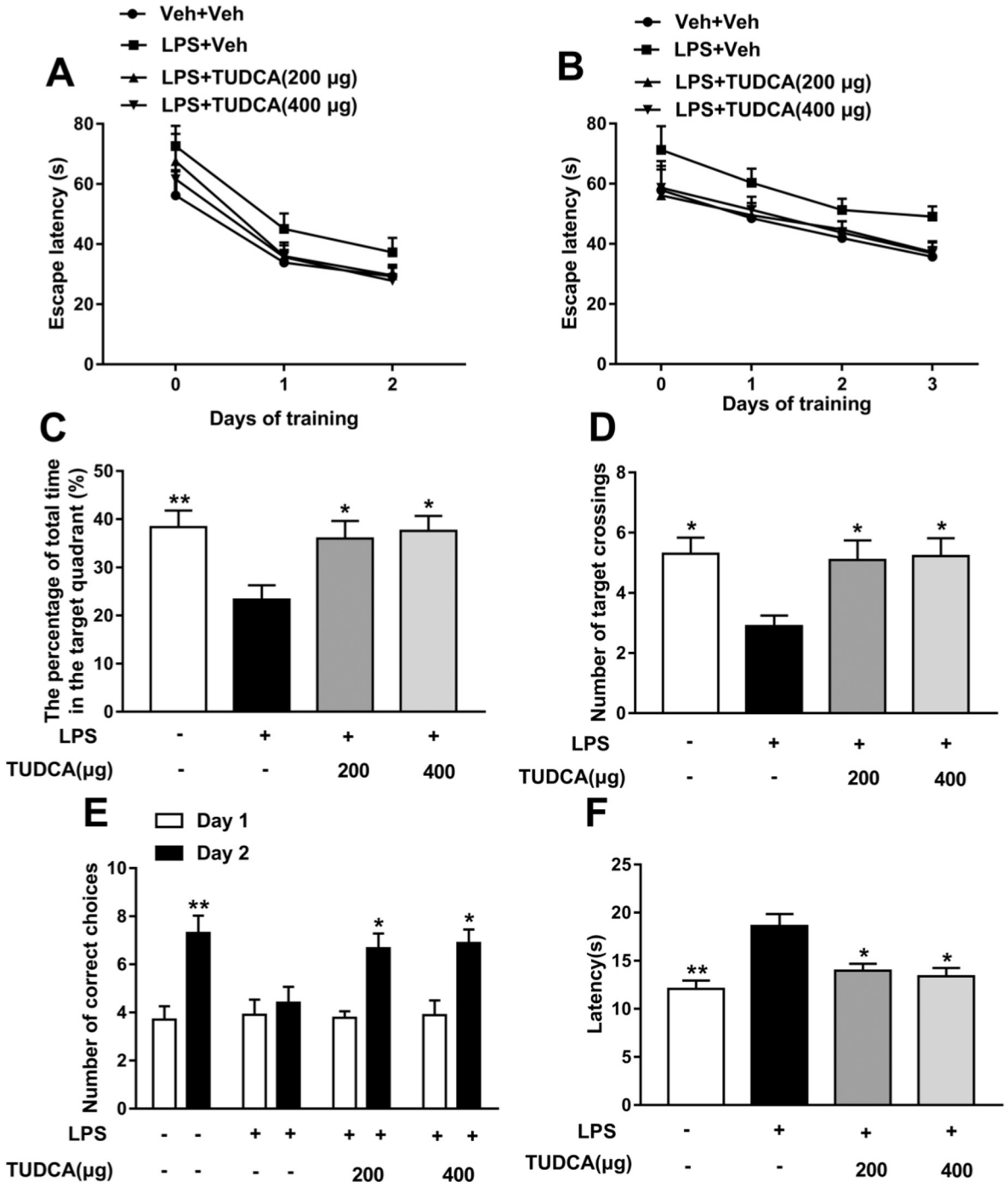

Fig. 2. TUDCA treatment ameliorated LPS-induced cognitive impairment in mice. (A) The mean escape latency (s) for mice searching for the visible platform in the Morris water maze test, day 0 indicates performance on the first trial and subsequent points represent the average of all daily trials. (B) The mean escape latency (s) to the hidden platform. (C) The percentage of time spent in the target quadrant and (D) the numbers of platform location crossings during the probe test on day 6. (E) The number of correct choices from day 1 to day 2 and (F) the mean latency (s) to enter the shock-free arm on day 2 were shown. Data are mean ± SEM, n = 12 mice/group. $^{*}P < 0.05$, $^{**}P < 0.01$ vs. LPS + Veh group.

Signaling Technology), BDNF (1:1000 dilution, Santa Cruz Biotechnology), PSD-95 (1:1000 dilution, Cell Signaling Technology), synaptophysin (1:1000 dilution, Cell Signaling Technology), β-actin (1:2000 dilution, Bioworld Technology) and Histone H3 (1:500 dilution, Bioworld Technology). Nucleoprotein was extracted using a nucleoprotein extraction kit (Sangon Biotech, China). The supernatant was used to detect the nuclear translocation of NF-κB p65 (1:1000 dilution, Cell Signaling Technology). The densitometry of immunoblot bands was measured using Image-J.

2.4. Immunohistochemistry

The brains were postfixed in 4% paraformaldehyde for 1 day and then transferred into 30% sucrose at 4 °C. Coronal sections (30 μm) were cut on a cryostat (Leica Microsystems, Germany). The sections were soaked in 3% H_2O_2 for 30 min. Then, the sections were blocked with a blocking solution (0.3% TritonX-100 and 5% BSA dissolved in PBS) for 1 h. Subsequently, the sections were incubated with the primary antibody for Iba1 (1:1000) overnight at 4 °C. Next day, the

sections were incubated with biotinylated mouse anti-rabbit lgG at 37 °C for 20 min, then incubated with streptavidin-biltin complex (SABC) for 30 min. Diaminobenzidine (DAB) was added to the sections followed by gradient dehydration. Then, soaked in xylene for 5 min to make it more transparent. The numbers of microglia cells in the hippocampal CA1, CA3 and DG regions were counted by Image-Pro Plus software version 6.0. In an average, 4 sections per mouse were used for statistical analysis.

2.5. Measurement of apoptotic cells

TUNEL staining was performed according to the manufacturer's protocol (Roche, Germany). Briefly, sections were incubated with TUNEL mixture in a humidified chamber for 60 min at 37 °C. Then, the sections were incubated for 10 min in darkness for DAPI staining. $TUNEL^+$ cells were identified under a fluorescence microscope (Leica Microsystems AG, Germany) by the co-localization of both the TUNEL signal and DAPI. Photomicrographs were analyzed using the Image-Pro Plus software version 6.0.

2.6. Golgi-staining

The brains were stained using a Golgi-staining kit according to the manufacturer's instructions (FD Neurotechnologies, Baltimore, MD, USA). The unfixed brains were submerged in the impregnation solution containing solution A and B (1:1) for 14 days and then removed to solution C for 3 days in the dark. 100 μm coronal sections were cut with a vibratome (Leica CM1950; Leica Microsystems, Germany). Then, the sections were stained with a mixed solution consisting of solution C, solution D and distilled water at 1:1:2 for 5 min. Next, the section was dehydrated in graded alcohol solutions and cleared in xylene. Images for neurons in the hippocampal DG region were obtained with a microscope at 1000× magnification (DM6000 B; Leica, Germany). The number of dendritic spines for each neuron was counted using Image J software.

2.7. Statistical analysis

Statistical analysis was performed using SPSS software (version 20.0; IBM, Armonk, NY). Behavioral data of Morris water maze was analyzed using two-way analysis of variance (treatment × trial time) with repeated measures (trial days) followed by Dunnett's post-hoc analysis. The other data were analyzed by one-way ANOVA followed by Dunnett's post-hoc analysis for multiple comparisons. Data are presented as the mean ± standard error of the mean (SEM), and P values < 0.05 were considered to be statistically significant.

3. Results

3.1. TUDCA treatment ameliorated cognitive deficits induced by LPS in mice

In order to avoid the possible influence of altered motor ability on cognitive function, the locomotor activity test was conducted at first. One-way ANOVA showed that no significant differences were detected between groups, including the distance traveled (F [3, 44] = 0.86, P = 0.47; Fig. 1B), the time spend in the center (F [3, 44] = 0.30, P = 0.83; Fig. 1C) and the average speed (F [3, 44] = 0.55, P = 0.65; Fig. 1D). Next, we evaluated the performance of mice in the MWM test. The data showed that the escape latency of mice in each group had no significant difference during the visible-platform training (days 1–2), suggesting that neither LPS nor TUDCA has any influence on basal motivation in mice. (effect of day, F [3, 428] = 40.12, P < 0.01; effect of group, F [3, 428] = 2.59, P > 0.05; effect of group-by-day interaction, F [3, 428] = 2.21, P > 0.05; Fig. 2A). As shown in Fig. 2B, LPS-treated mice had an increase in the escape latency in the hidden platform training (days 3–5) compared to animals exposed only to PBS. Treatment with TUDCA (200 or 400 μg) reversed this LPS-induced cognitive impairment and significantly decreasing the escape latency (effect of day, F [3, 620] = 13.40, P < 0.01; effect of group, F [3, 620] = 5.00, P > 0.05; effect of group-by-day interaction, F [3, 620] = 4.10, P > 0.05; Fig. 2B). In addition, TUDCA treatment displayed a significant increase in the percentage of total time spent in the target quadrant and the number of target crossings during the probe test (Fig. 2C and D). There were no significant differences in swimming speed between groups throughout the test (data not shown).

Additionally, mouse memory was evaluated in a Y-maze avoidance test. On day 1 (learning trial), there was no significant difference among all groups when the mice entered the compartment randomly (F [3, 44] = 2.15, P > 0.05; Fig. 2E). On day 2 (testing trial), the number of correct choices increased significantly in mice after treatment with TUDCA, meanwhile, the latency to enter the safe arm notably decreased compared with that of the mice treated with LPS (number of correct choices, F [3, 44] = 2.61, P < 0.01, Fig. 2E; the latency to enter the safe arm, F [3, 44] = 3.10, P < 0.01, Fig. 2F).

3.2. Hippocampal TGR5 expression was down-regulated by LPS exposure in mice and reversed by TUDCA treatment

To evaluate the effects of TUDCA on the expression of TGR5 in the hippocampus after LPS exposure, the level of TGR5 protein was detected using western blot. Immunoblot results showed lower protein level of TGR5 in the hippocampus of LPS-treated mice than that in the control. Interestingly, treatment with TUDCA dramatically blocked this decrease in the hippocampus (F [3, 8] = 3.91, P < 0.05; Fig. 3A and B).

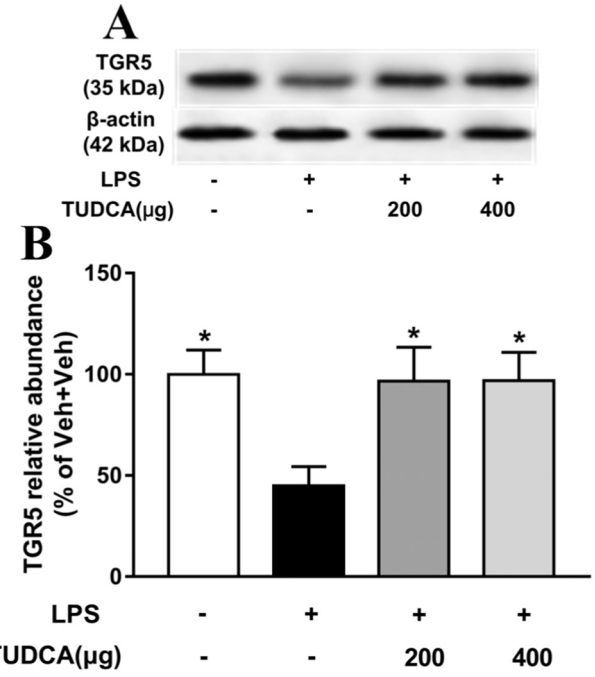

Fig. 3. TGR5 expression was down-regulated by LPS exposure in the hippocampus of mice and reversed by TUDCA treatment. (A) Representative immunoblots images for TGR5 in the hippocampus, and β-actin protein was used here as an internal control. (B) Quantification of TGR5 was expressed as the ratio (in percentage) of Veh + Veh group. Data are mean ± SEM, n = 3 mice/group. $^*P$ < 0.05, $^{**}P$ < 0.01 vs. LPS + Veh group.

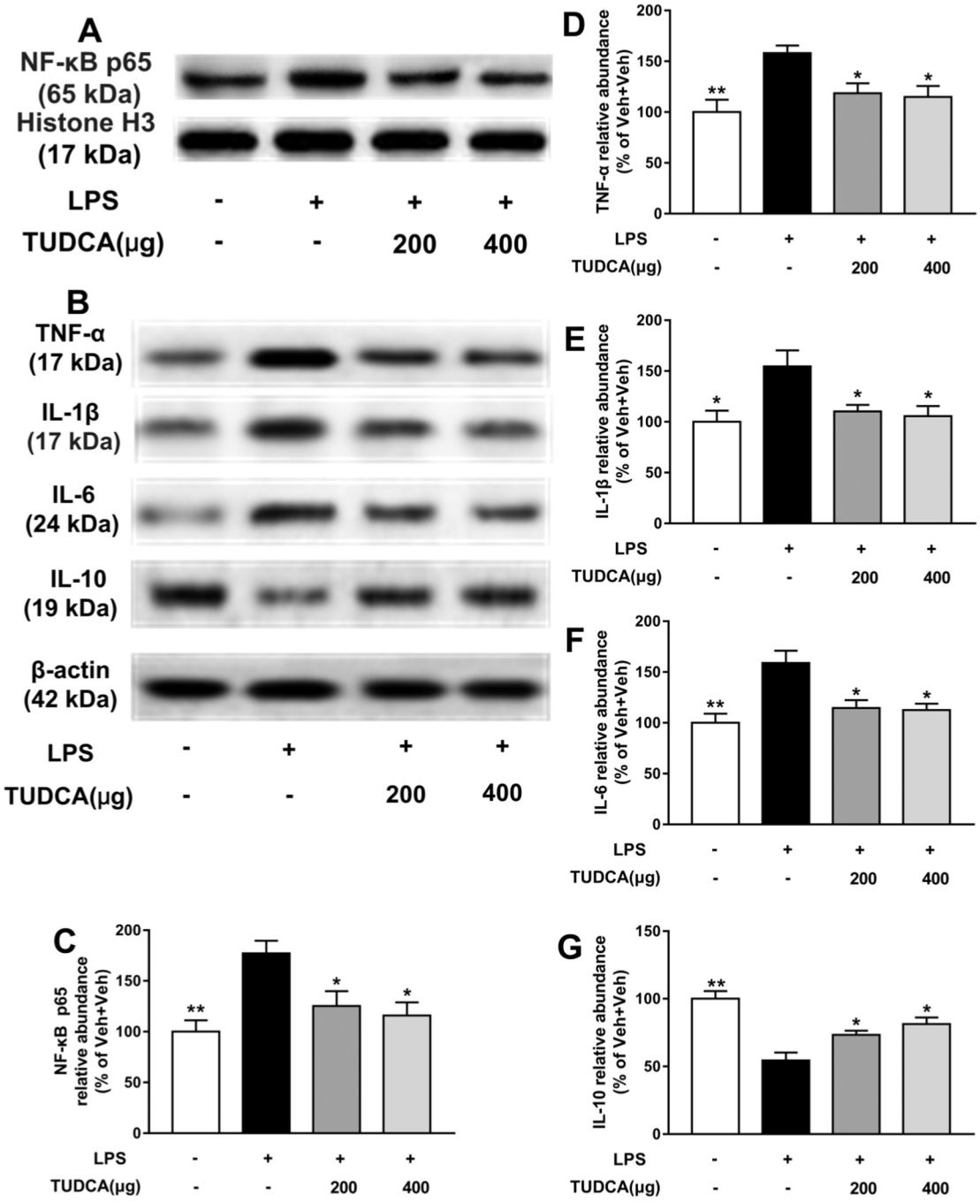

Fig. 4. TUDCA treatment suppressed LPS-activated NF-κB signaling and the production of proinflammatory cytokines. (A) Representative immunoblots of the nuclear NF-κB p65 in the hippocampus was shown, and Histone H3 was used as a loading control. (B) Representative immunoblots of TNF-α, IL-1β, IL-6 and IL-10 in the hippocampus, and β-actin protein was used here as an internal control. (C) Quantification of NF-κB p65 was expressed as the ratio (in percentage) of Veh + Veh group. Quantifications of (D) TNF-α, (E) IL-1β, (F) IL-6 and (G) IL-10 were expressed as the ratio (in percentage) of Veh + Veh group. Data are mean ± SEM, n = 3 mice/group. $^{*}P < 0.05$, $^{**}P < 0.01$ vs. LPS + Veh group.

3.3. TUDCA reversed upregulation of pro-inflammatory cytokines and downregulation of anti-inflammatory cytokines via NF-κB pathway in LPS-treated mice

LPS activated the NF-κB pathway by selectively inducing the nuclear translocation of p65 subunit [9,30]. Here, our data showed that the NF-κB p65 protein level was significantly increased in the hippocampus after LPS exposure, which was prevented by TUDCA treatment (F [3, 8] = 6.69, $P < 0.01$; Fig. 4A and C). The expression of the proinflammatory cytokines (TNF-α, IL-1β, and IL-6) in the hippocampus was also increased due to LPS exposure (Fig. 4B), TUDCA treatment significantly reduced their levels (F [3, 8] = 5.86, $P < 0.01$ for TNF-α, Fig. 4D; F [3, 8] = 4.81, $P < 0.05$ for IL-1β, Fig. 4E; F [3, 8] = 7.92, $P < 0.01$ for IL-6, Fig. 4F). In addition, the expression of anti-inflammatory cytokine IL-10 in the hippocampus was decreased after LPS exposure (F [3, 8] = 5.86, $P < 0.01$), while TUDCA treatment significantly increased its level ($P < 0.05$; Fig. 4B and G).

3.4. TUDCA treatment attenuated activation of microglia in the hippocampus of the LPS-treated mice

Neuroinflammation has been reported to be implicated in microglia

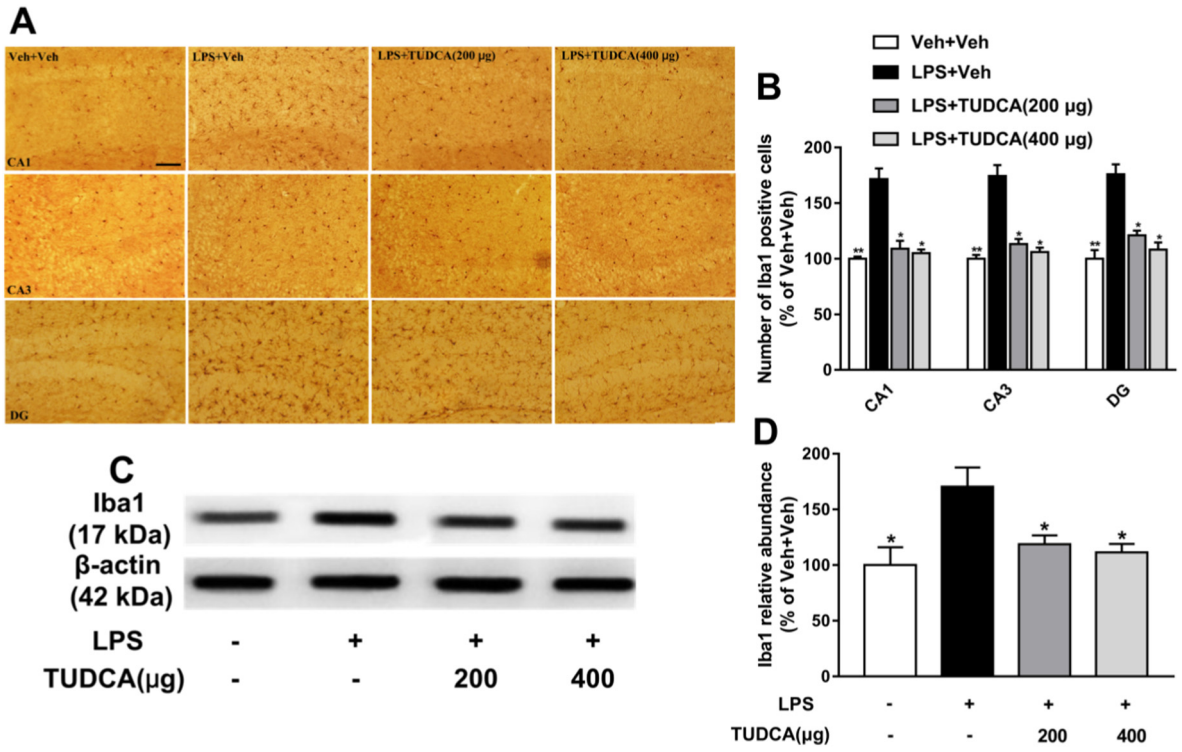

Fig. 5. TUDCA treatment attenuated the activation of microglia in the hippocampus of the LPS-treated mice. (A) Representative images of Iba1-labeled activated microglia in the hippocampal CA1, CA3 and DG regions. Original magnifications are 200× (Scale bar = 100 μm). (B) Quantification of the Iba1-positive cells in the hippocampal CA1, CA3 and DG regions, as the ratio (in percentage) of the Veh + Veh are shown. (C) Representative immunoblots of Iba1 in the hippocampus, and β-actin protein was used here as an internal control. (D) Quantifications of Iba1 was expressed as the ratio (in percentage) of Veh + Veh group. Data are mean ± SEM, n = 3 mice/group. $^{*}P < 0.05$, $^{**}P < 0.01$ vs. LPS + Veh group.

activation [2]. Our date showed that LPS caused obvious microglia activation labeled by Iba1 in the hippocampal CA1, CA3 and DG regions compared to the control group ($P < 0.01$, Fig. 5A and B). TUDCA treatment produced a significant decrease in the number of Iba1-positive cells compared to the LPS-treated group ($P < 0.05$; Fig. 5B). We also detected Iba1 level in the hippocampus using western blot. Consistent with the immunohistochemistry results, the level of Iba1 was also significantly elevated in the LPS-treated group (F [3, 8] = 5.68, $P < 0.05$; Fig. 5C and D), which was suppressed by TUDCA treatment ($P < 0.05$; Fig. 5C and D).

3.5. TUDCA treatment alleviated cell apoptosis triggered by LPS in the hippocampus

Our data showed that LPS caused a significant increase in TUNEL-positive cells in the hippocampal CA1, CA3, DG regions compared with the control group. Nevertheless, TUDCA treatment dramatically blocked this increase ($P < 0.01$, Fig. 6A and B). The anti-apoptotic effects of TUDCA were further studied using a western blot assay. The results showed that the expression of active caspase-3 was induced by LPS but decreased by TUDCA treatment (F [3, 8] = 6.26, $P < 0.01$, Fig. 6C and D). In addition, LPS exposure caused a down-regulation of the anti-apoptotic to pro-apoptotic molecules (Bcl-2/Bax) ratio, and treatment with TUDCA dramatically blocked this decrease in the hippocampus (Bcl-2/Bax: F [3, 8] = 5.61, $P < 0.01$; Fig. 6C and E).

3.6. TUDCA treatment increased the ratio of mBDNF/proBDNF in the hippocampus of LPS-treated mice

BDNF is synthesized as processor BDNF (proBDNF), and then cleaved into mature BDNF (mBDNF) within the endoplasmic reticulum, which plays an important role in memory. Our results showed that the ratio of mBDNF/proBDNF in the hippocampus was significantly decreased in the group of LPS + Veh, which was reversed by TUDCA treatment (F [3, 12] = 8.88, $P < 0.01$, Fig. 7A and B).

3.7. TUDCA treatment alleviated LPS-induced synaptic dysfunction in the hippocampus

Golgi staining showed that LPS exposure evoked damages of neuronal plasticity characterized by the obvious reduction in the number of spines, while TUDCA treatment dramatically restored the density of protrusions along the dendrite ($P < 0.05$, Fig. 8A and B). In addition, western blot analysis showed a significant reduction in PSD-95 and synaptophysin levels in LPS-treated mice (PSD-95: F [3, 8] = 8.87, $P < 0.01$, Fig. 8C and D; synaptophysin: F [3, 8] = 7.64, $P < 0.01$, Fig. 8C and E) but TUDCA treatment inhibited LPS-induced decrease in the expression of PSD-95 and synaptophysin protein ($P < 0.05$, Fig. 8D and E).

4. Discussion

Our data indicated that LPS treatment caused cognitive impairment, as evidenced by impaired performance in the Morris water maze and Y-maze avoidance tests. Moreover, LPS treatment in mice decreased TGR5 protein, elevated pro-inflammatory cytokines, reduced the production of the anti-inflammatory cytokines and activated microglia cells in the hippocampus by NF-κB signaling. It also increased the TUNEL-positive cells, activation of caspase-3 and decreased the ratio of Bcl-2/Bax or mBDNF/proBDNF, reduced the number of dendritic spines and the expression of synaptic proteins in the hippocampus. However, TUDCA (200 or 400 μg) treatment significantly inhibited such adverse cognitive and biochemical changes induced by LPS. Taken together, our results suggested that the neuroprotective role of TUDCA on LPS-induced

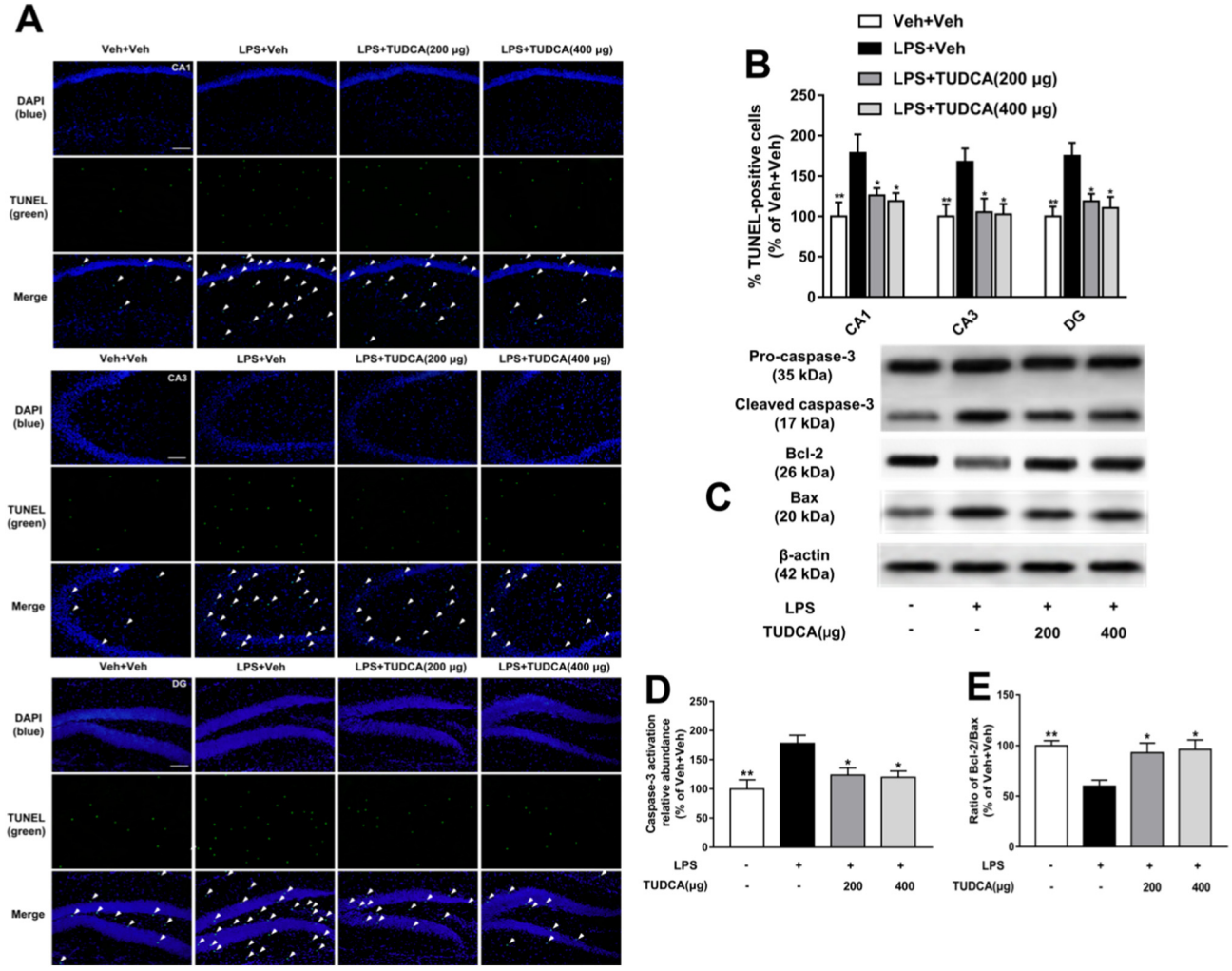

Fig. 6. TUDCA treatment alleviated neuronal apoptosis triggered by LPS in the hippocampus of mice. (A) Representative photomicrograph showing TUNEL-positive cells in the hippocampal CA1, CA3 and DG regions and arrows point to apoptotic cells. Scale bar = 100 μm. (B) The apoptotic bodies were expressed as a percentage of the total number of cells. (C) Representative immunoblots of pro-caspase-3, cleaved caspase-3, Bcl-2 and Bax in the hippocampus, and β-actin protein was used here as an internal control. (D) Caspase-3 activation was expressed as the ratio of caspase-3 fragment to pro-caspase-3. (E) The ratio of Bcl-2/Bax was expressed as the ratio (in percentage) of Veh + Veh group. Data are mean ± SEM, n = 3 mice/group. $^{*}P < 0.05$, $^{**}P < 0.01$ vs. LPS + Veh group.

cognitive impairment and neurotoxicity could be correlated with TGR5-mediated NF-κB signaling.

As reported previously, LPS is widely used to induce neuroinflammation, cognitive impairment and learning deficits [31,32]. Single intracerebroventricular injection of LPS can induce cognitive impairment and neurotoxicity in mice, thus modeling AD symptomatology [7]. The mechanisms involved in LPS-induced cognitive impairment and neurotoxicity are not fully understood. TGR5 agonists have been reported to reduce inflammation in an animal model of acute brain inflammation [24,33]. TUDCA is an endogenous hydrophilic bile acid with strong anti-apoptotic properties [34]. The anti-inflammatory properties of TUDCA in LPS induced neuroinflammation has been already reported [24], and this study is specifically focused on the protective effects of TUDCA in LPS-induced cognitive impairment. TGR5 mRNA expression has been detected in mouse brain, and activation of TGR5 can regulate bile acid homeostasis and glucose metabolism [18,20]. In addition, TGR5 activation also suppressed NF-κB-mediated inflammation through inhibiting nuclear translocation of p65 [35]. The p65 subunit is important and activation of the NF-κB target genes require its nuclear translocation [9,36]. The present results showed that TUDCA could downregulate the expression of NF-κB p65 and pro-inflammatory cytokines induced by LPS in the hippocampus. IL-10 appears to be a very important regulator of inflammation [37]. In contrast, IL-10, the expression level was significantly down-regulated in the LPS group, whereas TUDCA treatment significantly up-regulated its expression level. Neuroinflammation is associated with the activation of microglia cells [38]. Actually, microglia can produce various proinflammatory cytokines, including TNF-α, IL-1β and IL-6 after LPS exposure [39,40]. Therefore, inhibition of the activation of microglia and the consequent release of proinflammatory cytokines is seen as an important therapeutic strategy for AD. Our research showed that treatment with TUDCA efficiently suppressed the microglia activation in the hippocampal DG region induced by LPS.

Mounting evidence suggests that neuronal apoptosis is one of the important pathological features of cognitive impairment [41,42]. Zhuang et al. reported that activation of TGR5 increased expression of Bcl-2 and inhibited expressions of cleaved caspase-3 [43]. Our previous results have proved that LPS can induce apoptotic responses in the hippocampus [13]. The present results also showed that LPS triggered apoptotic response, upregulated the expression of caspase-3 and downregulated the Bcl-2/Bax ratio, leading to marked apoptotic responses in the hippocampus. Treatment with TUDCA significantly alleviated cell apoptosis triggered by LPS in the hippocampus (Fig. 6.). BDNF affects neurons bilaterally by the transition of proBDNF, the neurotoxic form of BDNF, to mBDNF, which enhances the synaptic plasticity and neuronal survival [44]. Our results show that the level of

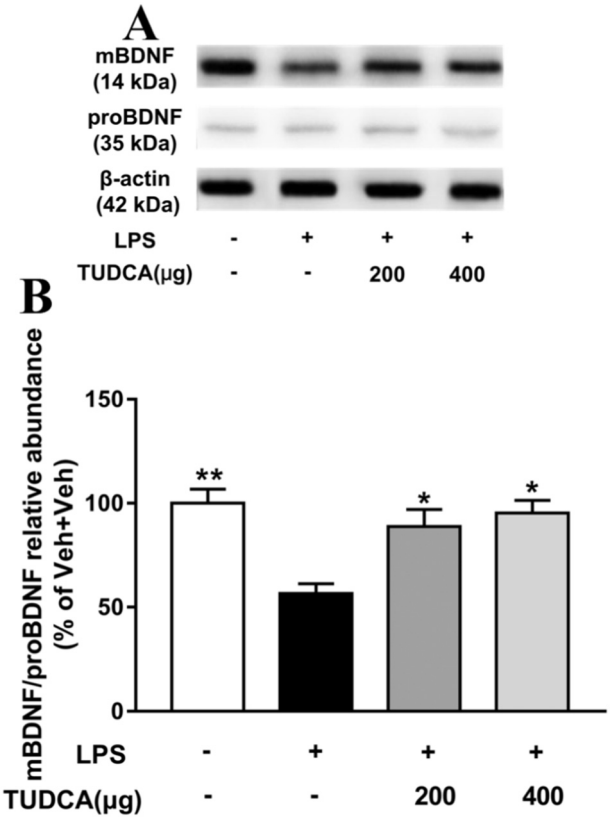

Fig. 7. TUDCA treatment increased the ratio of mBDNF/proBDNF in the hippocampus of LPS-treated mice. (A) Representative immunoblots of mBDNF and proBDNF. β-actin was used as a loading control. (B) The ratio of mBDNF/proBDNF was expressed as the ratio (in percentage) of Veh + Veh group are shown. Data are mean ± SEM, n = 3 mice/group. $^{*}P < 0.05$, $^{**}P < 0.01$ vs. LPS + Veh group.

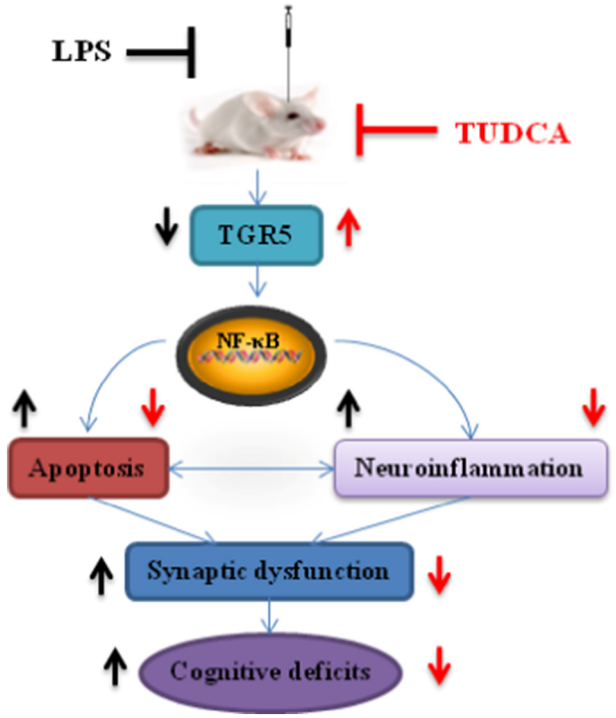

Fig. 9. Schematic representation illustrating the mechanism of TUDCA on its neuroprotective effects.

mBDNF was decreased in the LPS-treated mice, which was reversed by TUDCA treatment. Therefore, the regulation of mature BDNF expression was considered beneficial for the therapy of AD.

A number of investigators reported that cognitive impairment is associated with the synaptic loss in the hippocampus [5,45]. In line with previous studies, LPS-induced the loss of dendrites spines in the

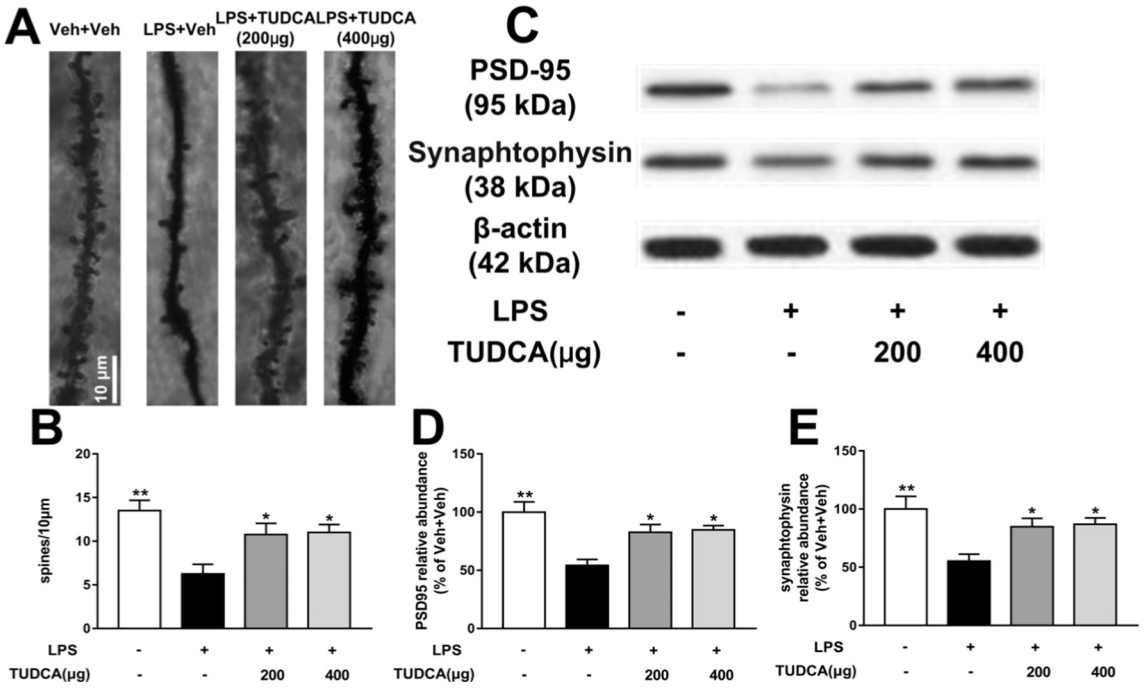

Fig. 8. TUDCA treatment alleviated LPS-induced synaptic dysfunction in the hippocampus of mice. (A) Representative dendritic spine images from the hippocampal DG region. Scale bar is 10 μm. (B) Statistical analysis of the average number of Golgi stained dendritic spines. (C) Representative immunoblots of PSD-95 and synaptophysin, and β-actin protein was used here as an internal control. Quantitative analysis of (D) PSD-95 and (E) synaptophysin was expressed as the ratio (in percentage) of Veh + Veh group. Data are mean ± SEM, n = 3 mice/group. $^{*}P < 0.05$, $^{**}P < 0.01$ vs. LPS + Veh group.

hippocampus [46]. Golgi staining disclosed that TUDCA treatment could significantly increase the number of spines (Fig. 8A). PSD-95 and synaptophysin levels have been also found to be decreased in the brains of AD [47,48]. The scaffolding protein PSD-95 is significantly decreased due to LPS exposure. The similar diminishing is observed in the dominant presynaptic vesicle protein marker, synaptophysin [49]. In this study, treatment with TUDCA ameliorated the loss of these two dominant synaptic proteins caused by LPS.

To sum up, our data showed that TUDCA ameliorated cognitive impairment, neuroinflammation, neuroapoptosis and synaptic dysfunction induced by LPS, which is involved in TGR5-mediated NF-κB signaling (Fig. 9). Accordingly, TUDCA might be a promising new therapeutic agent for the treatment of AD.

Acknowledgements

This work was supported by the Natural Science Foundation of China (81573413, 81273497 and 81773714 to Hao Hong, 81603113 to Su Su Tang), Postgraduate Research & Practice Innovation Program of Jiangsu Province (KYCX18_0764), and the Fundamental Research Funds for the Central Universities (2632017PT01).

Competing interests

The authors declare that they have no competing interests.

References

[1] R.B. Maccioni, L.E. Rojo, J.A. Fernandez, R.O. Kuljis, The role of neuroimmunomodulation in Alzheimer's disease, Ann. N. Y. Acad. Sci. 1153 (2009) 240–246.
[2] X. Deng, M. Li, W. Ai, L. He, D. Lu, P.R. Patrylo, H. Cai, X. Luo, Z. Li, X. Yan, Lipolysaccharide-induced neuroinflammation is associated with Alzheimer-like amyloidogenic axonal pathology and dendritic degeneration in rats, Adv. Alzheimers Dis. 3 (2) (2014) 78–93.
[3] F. Ali, M.S. Hossain, S. Sejimo, K. Akashi, Plasmalogens inhibit endocytosis of toll-like receptor 4 to attenuate the inflammatory signal in microglial cells, Mol. Neurobiol. (2018), https://doi.org/10.1007/s12035-018-1307-2.
[4] L.T. Tien, Y.J. Lee, Y. Pang, S. Lu, J.W. Lee, C.H. Tseng, A.J. Bhatt, R.D. Savich, L.W. Fan, Neuroprotective effects of intranasal IGF-1 against neonatal lipopolysaccharide-induced neurobehavioral deficits and neuronal inflammation in the substantia nigra and locus coeruleus of juvenile rats, Dev. Neurosci. 39 (6) (2017) 443–459.
[5] Y. Liu, Y. Zhang, X. Zheng, T. Fang, X. Yang, X. Luo, A. Guo, K.A. Newell, X.F. Huang, Y. Yu, Galantamine improves cognition, hippocampal inflammation, and synaptic plasticity impairments induced by lipopolysaccharide in mice, J. Neuroinflammation 15 (1) (2018) 112.
[6] Y. Nadler, A. Alexandrovich, N. Grigoriadis, T. Hartmann, K.S. Rao, E. Shohami, R. Stein, Increased expression of the gamma-secretase components presenilin-1 and nicastrin in activated astrocytes and microglia following traumatic brain injury, Glia 56 (5) (2008) 552–567.
[7] X.Y. Zhang, J.B. Cao, L.M. Zhang, Y.F. Li, W.D. Mi, Deferoxamine attenuates lipopolysaccharide-induced neuroinflammation and memory impairment in mice, J. Neuroinflammation 12 (2015) 20.
[8] M.A. Faris, S. Kacimi, R.A. Al-Kurd, M.A. Fararjeh, Y.K. Bustanji, M.K. Mohammad, M.L. Salem, Intermittent fasting during Ramadan attenuates proinflammatory cytokines and immune cells in healthy subjects, Nutr. Res. 32 (12) (2012) 947–955.
[9] E.A.M. El-Shoura, B.A.S. Messiha, S.M.Z. Sharkawi, R.A.M. Hemeida, Perindopril ameliorates lipopolysaccharide-induced brain injury through modulation of angiotensin-II/angiotensin-1-7 and related signaling pathways, Eur. J. Pharmacol. 834 (2018) 305–317.
[10] J.S. Jacobsen, C.C. Wu, J.M. Redwine, T.A. Comery, R. Arias, M. Bowlby, R. Martone, J.H. Morrison, M.N. Pangalos, P.H. Reinhart, F.E. Bloom, Early-onset behavioral and synaptic deficits in a mouse model of Alzheimer's disease, Proc. Natl. Acad. Sci. U. S. A. 103 (13) (2006) 5161–5166.
[11] P. Edison, C.K. Donat, M. Sastre, In vivo imaging of glial activation in Alzheimer's disease, Front. Neurol. 9 (2018) 625.
[12] S.N. Andy, V. Pandy, Z. Alias, H.A. Kadir, Deoxyelephantopin ameliorates lipopolysaccharides (LPS)-induced memory impairments in rats: evidence for its anti-neuroinflammatory properties, Life Sci. 206 (2018) 45–60.
[13] F. Chen, A. Ghosh, F. Wu, S. Tang, M. Hu, H. Sun, L. Kong, H. Hong, Preventive effect of genetic knockdown and pharmacological blockade of CysLT1R on lipopolysaccharide (LPS)-induced memory deficit and neurotoxicity in vivo, Brain Behav. Immun. 60 (2017) 255–269.
[14] P.K. Fruhauf-Perez, F.R. Temp, M.M. Pillat, C. Signor, A.L. Wendel, H. Ulrich, C.F. Mello, M.A. Rubin, Spermine protects from LPS-induced memory deficit via BDNF and TrkB activation, Neurobiol. Learn. Mem. 149 (2018) 135–143.
[15] S.A. Heldt, L. Stanek, J.P. Chhatwal, K.J. Ressler, Hippocampus-specific deletion of BDNF in adult mice impairs spatial memory and extinction of aversive memories, Mol. Psychiatry 12 (7) (2007) 656–670.
[16] J. Liu, L. Chang, F. Roselli, O.F. Almeida, X. Gao, X. Wang, D.T. Yew, Y. Wu, Amyloid-beta induces caspase-dependent loss of PSD-95 and synaptophysin through NMDA receptors, J. Alzheimers Dis. 22 (2) (2010) 541–556.
[17] D. Chugh, P. Nilsson, S.A. Afjei, A. Bakochi, C.T. Ekdahl, Brain inflammation induces post-synaptic changes during early synapse formation in adult-born hippocampal neurons, Exp. Neurol. 250 (2013) 176–188.
[18] M. McMillin, G. Frampton, R. Tobin, G. Dusio, J. Smith, H. Shin, K. Newell-Rogers, S. Grant, S. DeMorrow, TGR5 signaling reduces neuroinflammation during hepatic encephalopathy, J. Neurochem. 135 (3) (2015) 565–576.
[19] A. Perino, K. Schoonjans, TGR5 and immunometabolism: insights from physiology and pharmacology, Trends Pharmacol. Sci. 36 (12) (2015) 847–857.
[20] V. Keitel, B. Gorg, H.J. Bidmon, I. Zemtsova, L. Spomer, K. Zilles, D. Haussinger, The bile acid receptor TGR5 (Gpbar-1) acts as a neurosteroid receptor in brain, Glia 58 (15) (2010) 1794–1805.
[21] M. Lasalle, V. Hoguet, N. Hennuyer, F. Leroux, C. Piveteau, L. Belloy, S. Lestavel, E. Vallez, E. Dorchies, I. Duplan, E. Sevin, M. Culot, F. Gosselet, R. Boulahjar, A. Herledan, B. Staels, B. Deprez, A. Tailleux, J. Charton, Topical intestinal aminoimidazole agonists of G-protein-coupled bile acid receptor 1 promote glucagon like peptide-1 secretion and improve glucose tolerance, J. Med. Chem. 60 (10) (2017) 4185–4211.
[22] D.D. Yu, K.M. Sousa, D.L. Mattern, J. Wagner, X. Fu, N. Vaidehi, B.M. Forman, W. Huang, Stereoselective synthesis, biological evaluation, and modeling of novel bile acid-derived G-protein coupled bile acid receptor 1 (GP-BAR1, TGR5) agonists, Bioorg. Med. Chem. 23 (7) (2015) 1613–1628.
[23] C.M. Rodrigues, S. Sola, Z. Nan, R.E. Castro, P.S. Ribeiro, W.C. Low, C.J. Steer, Tauroursodeoxycholic acid reduces apoptosis and protects against neurological injury after acute hemorrhagic stroke in rats, Proc. Natl. Acad. Sci. U. S. A. 100 (10) (2003) 6087–6092.
[24] N. Yanguas-Casas, M.A. Barreda-Manso, M. Nieto-Sampedro, L. Romero-Ramirez, TUDCA: an agonist of the bile acid receptor GPBAR1/TGR5 with anti-inflammatory effects in microglial cells, J. Cell. Physiol. 232 (8) (2017) 2231–2245.
[25] N. Yanguas-Casas, M.A. Barreda-Manso, M. Nieto-Sampedro, L. Romero-Ramirez, Tauroursodeoxycholic acid reduces glial cell activation in an animal model of acute neuroinflammation, J. Neuroinflammation 11 (2014) 50.
[26] S.P. Navabi, A. Sarkaki, E. Mansouri, M. Badavi, A. Ghadiri, Y. Farbood, The effects of betulinic acid on neurobehavioral activity, electrophysiology and histological changes in an animal model of the Alzheimer's disease, Behav. Brain Res. 337 (2018) 99–106.
[27] X. Wu, Y.G. Lv, Y.F. Du, M. Hu, M.N. Reed, Y. Long, V. Suppiramaniam, H. Hong, S.S. Tang, Inhibitory effect of INT-777 on lipopolysaccharide-induced cognitive impairment, neuroinflammation, apoptosis, and synaptic dysfunction in mice, Prog. Neuro-Psychopharmacol. Biol. Psychiatry 88 (2019) 360–374.
[28] S.S. Tang, H. Hong, L. Chen, Z.L. Mei, M.J. Ji, G.Q. Xiang, N. Li, H. Ji, Involvement of cysteinyl leukotriene receptor 1 in Abeta1-42-induced neurotoxicity in vitro and in vivo, Neurobiol. Aging 35 (3) (2014) 590–599.
[29] R. Morris, Developments of a water-maze procedure for studying spatial learning in the rat, J. Neurosci. Methods 11 (1) (1984) 47–60.
[30] T.D. Gilmore, Introduction to NF-kappaB: players, pathways, perspectives, Oncogene 25 (51) (2006) 6680–6684.
[31] J. Sun, S. Zhang, X. Zhang, X. Zhang, H. Dong, Y. Qian, IL-17A is implicated in lipopolysaccharide-induced neuroinflammation and cognitive impairment in aged rats via microglial activation, J. Neuroinflammation 12 (2015) 165.
[32] S. Rosi, A. Vazdarjanova, V. Ramirez-Amaya, P.F. Worley, C.A. Barnes, G.L. Wenk, Memantine protects against LPS-induced neuroinflammation, restores behaviorally-induced gene expression and spatial learning in the rat, Neuroscience 142 (4) (2006) 1303–1315.
[33] C. Guo, H. Qi, Y. Yu, Q. Zhang, J. Su, D. Yu, W. Huang, W.D. Chen, Y.D. Wang, The G-protein-coupled bile acid receptor Gpbar1 (TGR5) inhibits gastric inflammation through antagonizing NF-kappaB signaling pathway, Front. Pharmacol. 6 (2015) 287.
[34] R.M. Ramalho, P.S. Ribeiro, S. Sola, R.E. Castro, C.J. Steer, C.M. Rodrigues, Inhibition of the E2F-1/p53/Bax pathway by tauroursodeoxycholic acid in amyloid beta-peptide-induced apoptosis of PC12 cells, J. Neurochem. 90 (3) (2004) 567–575.
[35] J. Su, Q. Zhang, H. Qi, L. Wu, Y. Li, D. Yu, W. Huang, W.D. Chen, Y.D. Wang, The G-protein-coupled bile acid receptor Gpbar1 (TGR5) protects against renal inflammation and renal cancer cell proliferation and migration through antagonizing NF-kappaB and STAT3 signaling pathways, Oncotarget 8 (33) (2017) 54378–54387.
[36] P. Viatour, M.P. Merville, V. Bours, A. Chariot, Phosphorylation of NF-kappaB and IkappaB proteins: implications in cancer and inflammation, Trends Biochem. Sci. 30 (1) (2005) 43–52.
[37] L. Subedi, J.H. Lee, S. Yumnam, E. Ji, S.Y. Kim, Anti-inflammatory effect of sulforaphane on LPS-activated microglia potentially through JNK/AP-1/NF-kappaB inhibition and Nrf2/HO-1 activation, Cells 8 (2) (2019).
[38] I. Berkiks, S. Boulbaroud, L.M. Garcia-Segura, A. Mesfioui, A. Ouichou, S. Mouden, H. Benmhammed, A. El Hasnaoui, R. Nakache, Y. Bahbiti, A. El Hessni, Thymelaea lythroides extract attenuates microglial activation and depressive-like behavior in LPS-induced inflammation in adult male rats, Biomed. Pharmacother. 99 (2018) 655–663.
[39] L. Fu, P. Zhu, S. Qi, C. Li, K. Zhao, MicroRNA-92a antagonism attenuates lipopolysaccharide (LPS)-induced pulmonary inflammation and injury in mice through suppressing the PTEN/AKT/NF-kappaB signaling pathway, Biomed. Pharmacother. 107 (2018) 703–711.

[40] Z. Peng, X. Gong, Y. Yang, L. Huang, Q. Zhang, P. Zhang, R. Wan, B. Zhang, Hepatoprotective effect of quercetin against LPS/d-GalN induced acute liver injury in mice by inhibiting the IKK/NF-kappaB and MAPK signal pathways, Int. Immunopharmacol. 52 (2017) 281–289.

[41] P. Wei, Q. Liu, D. Li, Q. Zheng, J. Zhou, J. Li, Acute nicotine treatment attenuates lipopolysaccharide-induced cognitive dysfunction by increasing BDNF expression and inhibiting neuroinflammation in the rat hippocampus, Neurosci. Lett. 604 (2015) 161–166.

[42] J.W. Guo, P.P. Guan, W.Y. Ding, S.L. Wang, X.S. Huang, Z.Y. Wang, P. Wang, Erythrocyte membrane-encapsulated celecoxib improves the cognitive decline of Alzheimer's disease by concurrently inducing neurogenesis and reducing apoptosis in APP/PS1 transgenic mice, Biomaterials 145 (2017) 106–127.

[43] L. Zhuang, Y. Fan, L. Lu, W. Ding, C. Ni, X. Wang, F. Zhang, J. Rao, Ischemic preconditioning protects hepatocytes from ischemia-reperfusion injury via TGR5-mediated anti-apoptosis, Biochem. Biophys. Res. Commun. 473 (4) (2016) 966–972.

[44] L.C. Harte-Hargrove, N.J. Maclusky, H.E. Scharfman, Brain-derived neurotrophic factor-estrogen interactions in the hippocampal mossy fiber pathway: implications for normal brain function and disease, Neuroscience 239 (2013) 46–66.

[45] R.M. Barrientos, E.A. Higgins, J.C. Biedenkapp, D.B. Sprunger, K.J. Wright-Hardesty, L.R. Watkins, J.W. Rudy, S.F. Maier, Peripheral infection and aging interact to impair hippocampal memory consolidation, Neurobiol. Aging 27 (5) (2006) 723–732.

[46] J.C. Delpech, A. Thomazeau, C. Madore, C. Bosch-Bouju, T. Larrieu, C. Lacabanne, J. Remus-Borel, A. Aubert, C. Joffre, A. Nadjar, S. Laye, Dietary n-3 PUFAs deficiency increases vulnerability to inflammation-induced spatial memory impairment, Neuropsychopharmacology 40 (12) (2015) 2774–2787.

[47] C.I. Sze, J.C. Troncoso, C. Kawas, P. Mouton, D.L. Price, L.J. Martin, Loss of the presynaptic vesicle protein synaptophysin in hippocampus correlates with cognitive decline in Alzheimer disease, J. Neuropathol. Exp. Neurol. 56 (8) (1997) 933–944.

[48] D.H. Kim, H. Lim, D. Lee, S.J. Choi, W. Oh, Y.S. Yang, J.S. Oh, H.H. Hwang, H.B. Jeon, Thrombospondin-1 secreted by human umbilical cord blood-derived mesenchymal stem cells rescues neurons from synaptic dysfunction in Alzheimer's disease model, Sci. Rep. 8(1) (2018) 354.

[49] A. Ahmad, T. Ali, H.Y. Park, H. Badshah, S.U. Rehman, M.O. Kim, Neuroprotective effect of fisetin against amyloid-beta-induced cognitive/synaptic dysfunction, neuroinflammation, and neurodegeneration in adult mice, Mol. Neurobiol. 54 (3) (2017) 2269–2285.